Comparison of global climatological maps of sea surface dimethyl sulfide

Sauveur Belviso, L. Bopp, C. Moulin, James C. Orr, T.R. Anderson, Olivier Aumont, S. Chu, S. Elliott, M. E. Maltrud, R. Simó

Comparison of global climatological maps of sea surface dimethyl sulfide

S. Belviso,[1] L. Bopp,[1] C. Moulin,[1] J. C. Orr,[1] T. R. Anderson,[2] O. Aumont,[3] S. Chu,[4] S. Elliott,[4] M. E. Maltrud,[4] and R. Simó[5]

Received 21 November 2003; revised 19 April 2004; accepted 19 May 2004; published 21 August 2004.

[1] We have examined differences in regional and seasonal variability among seven global climatologies of sea-surface dimethyl sulfide (DMS) concentrations. We found large differences between recent climatologies and that typically used by most atmospheric sulfur models. The relative uncertainty (1σ/mean) in the latitudinal distribution of the annual mean DMS concentration increases from about 50% in tropical and temperate regions to nearly 100% in the high latitudes. We also compared these climatologies to new measurements in the North Atlantic Ocean taken during the 2001 Programme Océan Multidisciplinaire Méso Echelle (POMME) expeditions. *INDEX TERMS:* 1635 Global Change: Oceans (4203); 4263 Oceanography: General: Ocean prediction; 4805 Oceanography: Biological and Chemical: Biogeochemical cycles (1615); 4820 Oceanography: Biological and Chemical: Gases; *KEYWORDS:* biogeochemistry, DMS, DMSP

Citation: Belviso, S., L. Bopp, C. Moulin, J. C. Orr, T. R. Anderson, O. Aumont, S. Chu, S. Elliott, M. E. Maltrud, and R. Simó (2004), Comparison of global climatological maps of sea surface dimethyl sulfide, *Global Biogeochem. Cycles*, *18*, GB3013, doi:10.1029/2003GB002193.

1. Introduction

[2] Recent modeling studies suggest that dimethyl sulfide (DMS) and its atmospheric degradation products help regulate climate through two separate effects. First, these compounds influence cloud sensitivity to anthropogenic sulfate aerosols. For example, when DMS emissions are doubled in an atmospheric sulfur-climate model, there is a 25% reduction in the indirect radiative forcing due to anthropogenic sulfate aerosols [*Jones et al.*, 2001]. These increased DMS emissions result in higher background concentrations of natural sulfate aerosols and cloud condensation nucleii, which reduce cloud sensitivity to anthropogenic sulfate aerosols. Another atmospheric modeling study by *Boucher et al.* [2003] tested the sensitivity of results to DMS emissions from two different climatologies [*Kettle and Andreae*, 2000; *Aumont et al.*, 2002]. They found that a 5.5% increase in the global DMS emissions caused an 11.6% reduction in the first indirect radiative forcing due to anthropogenic sulfate aerosols. Thus, in a world with a higher atmospheric load of DMS-derived aerosols, polluted clouds would be less efficient in scattering solar radiation back to space.

[3] The second effect concerns cloud albedo in clean marine air [*Shaw*, 1983; *Charlson et al.*, 1987]. In a global warming scenario with doubled atmospheric CO_2 relative to present, the models of *Gabric et al.* [2001] and *Bopp et al.* [2003, 2004] simulate a significant negative radiative impact due to enhanced DMS production, particularly from the Southern Ocean. The increase in DMS emissions results in higher concentrations of sulfate aerosol and cloud condensation nuclei. In turn, this augments cloud albedo due to an increase in the cloud droplet number and a decrease in droplet size at constant cloud water content. There is also compelling observational evidence from the Southern Hemisphere that suggests that cloud optical properties respond to changes in cloud microphysical properties that appear to be determined by DMS and its atmospheric products [*Ayers and Gillett*, 2000; *Belviso et al.*, 2000]. To properly assess DMS feedback on the climate system, it is fundamental to establish the uncertainty to which we are able to assess the present-day distribution of sea-surface DMS.

[4] Since the pioneering studies of *Bates et al.* [1987], *Erickson et al.* [1990], and *Andreae* [1990], several new DMS monthly climatologies have been proposed [*Kettle et al.*, 1999; *Kettle and Andreae*, 2000; *Anderson et al.*, 2001; *Aumont et al.*, 2002; *Simó and Dachs*, 2002; *Chu et al.*, 2003; *Belviso et al.*, 2004]. Yet most atmospheric sulfur models have used only one reference, the climatology from *Kettle and Andreae* [2000]. Recently though, use of three sea-surface DMS climatologies [*Kettle and Andreae*, 2000; *Aumont et al.*, 2002; *Belviso et al.*, 2004] with one atmospheric model revealed large differences in terms of the

[1]Laboratoire des Sciences du Climat et de l'Environnement, Gif-sur-Yvette, France.
[2]Southampton Oceanography Center, Waterfront Campus, University of Southampton, Southampton, UK.
[3]Laboratoire d'Océanographie Dynamique et de Climatologie, Université Pierre et Marie Curie, Paris, France.
[4]Climate, Ocean and Sea Ice Modeling Project (COSIM), Los Alamos National Laboratory, Los Alamos, New Mexico, USA.
[5]Institut de Ciències del Mar (CMIMA-CSIC), Barcelona, Spain.

0886-6236/04/2003GB002193

Table 1. Climatologies Characteristics

	K99	K	A	O	S	C	B
References	*Kettle et al.* [1999]	*Kettle and Andreae* [2000]	*Anderson et al.* [2001]	*Aumont et al.* [2002]	*Simó and Dachs* [2002]	*Chu et al.* [2003]	*Belviso et al.* [2004]
Horizontal resolution (lon. × lat.)	1° × 1°	1° × 1°	0.5° × 0.5°	2° × 0.5–2°	0.5° × 0.5°	0.28° × 0.28 cos(lat.)	1° × 1°
Methods	compilation of DMS data Extrapolations Interpolations	updated compilation of DMS data Extrapolations Interpolations	parameterizations	process model Parameterizations	parameterizations	process model	parameterizations
Proxies of DMS			Chl *a* (SeaWiFS) nitrates (Levitus) light [*Esbensen and Kushnir*, 1981]	Chl *a* (model) Fp-ratio (model)	Chl *a* (SeaWiFS) MLD (Levitus)		Chl *a* (SeaWiFS) Fp-ratio (related to Chl *a*)
Annual mean DMS, nmol L^{-1}	2.13	2.01	2.55	1.70	2.28	1.51	1.60

ability to match observed spatiotemporal distributions of DMS and sulfur dioxide in the marine atmosphere [*Boucher et al.*, 2003, Figure 5]. Here our first goal was to quantify the differences between the existing global climatologies of sea-surface DMS, thus providing some measure of uncertainty. Second, we aimed to quantify the extent to which these climatologies were able to match observations of sea-surface DMS in different oceanic regions.

2. Description of the Global Fields of DMS

[5] The general characteristics of the seven global-scale climatologies are presented in Table 1. In the first two studies, *Kettle et al.* [1999] and *Kettle and Andreae* [2000] began with a database of over 15,000 DMS measurements, nonrandomly distributed in space and time. They then used a complex set of extrapolations, interpolations, and iterations to derive monthly climatological maps of sea-surface DMS. By definition, results at any given grid cell are not identical to the field data. In a third study, *Anderson et al.* [2001] also relied on the *Kettle et al.* [1999] database of surface DMS measurements, but they chose to use a simple empirical relationship (''broken-stick'' regression) to compute DMS from chlorophyll, light, and nutrients. Their approach yields high concentrations of DMS in the high latitude, but it underestimates DMS variability in low-DMS areas. In a fourth study, *Simó and Dachs* [2002] once again relied on the *Kettle et al.* [1999] database; however, they developed a two-equation algorithm, which was found to explain a large fraction of the variance of sea-surface DMS concentration. Their algorithm produces monthly global maps of DMS concentration from surface chlorophyll (Sea-viewing Wide Field-of-view Sensor (SeaWiFS)) and mixed layer depth (MLD) climatology from National Oceanic and Atmospheric Administration (NOAA). In a fifth study, *Belviso et al.* [2004] used nonlinear parameterizations to compute DMS concentrations from chlorophyll (from SeaWiFS) and an index of the community structure of marine phytoplankton, the Fp-ratio, which represents the proportion of micro-phytoplankton within the whole phytoplankton community. An upper cut-off for the chlorophyll-derived DMS concentration was limited to 50 nmol L^{-1} to overcome unrealistically large values in coastal waters. With this method, no DMS predictions were possible at high latitudes in winter because SeaWiFS observations are limited to ice-free regions with sufficient solar irradiance. The background DMS level was therefore set to 0.2 nmol L^{-1} in these regions. In a sixth approach, *Aumont et al.* [2002] used analogous nonlinear relationships, but their fields for chlorophyll and the index for community structure were derived from a global ocean biogeochemical model. In a seventh approach, *Chu et al.* [2003] developed a prognostic biogeochemical formulation for production and removal of DMS and made simulations with that in a high-resolution ocean circulation model (Parallel Ocean Program). Dissolved dimethylsulfoniopropionate (DMSPd), the principal precursor of DMS in the model of *Chu et al.* [2003], is produced by planktonic excretion of DMSP and consumed by bacterial assimilation and phytoplanktonic and bacterial DMSP-lyase activity. Direct excretion of DMS by phytoplankton and lysis of DMSPd yields DMS that is removed by bacterial consumption, photolysis, and gas exchange at the air-sea interface.

3. Results

[6] For a concise summary of differences between each global DMS climatology and the typical reference K [*Kettle and Andreae*, 2000], we used *Taylor*'s [2001] diagram that simultaneously compares several frequently used statistics (Figure 1): the standard deviation, the correlation coefficient *r*, and the pattern root mean square (RMS) error. The overall variance for the B [*Belviso et al.*, 2004] and S [*Simó and Dachs*, 2002] climatologies is similar to that for the reference (K). Slightly greater variance is exhibited by the older K99 climatology [*Kettle et al.*, 1999], whereas substantially less variance is found for the A [*Anderson et al.*, 2001], O [*Aumont et al.*, 2002], and C [*Chu et al.*, 2003] climatologies. Although overall variability may be similar, this does not necessarily mean that it is collocated, hence the interest

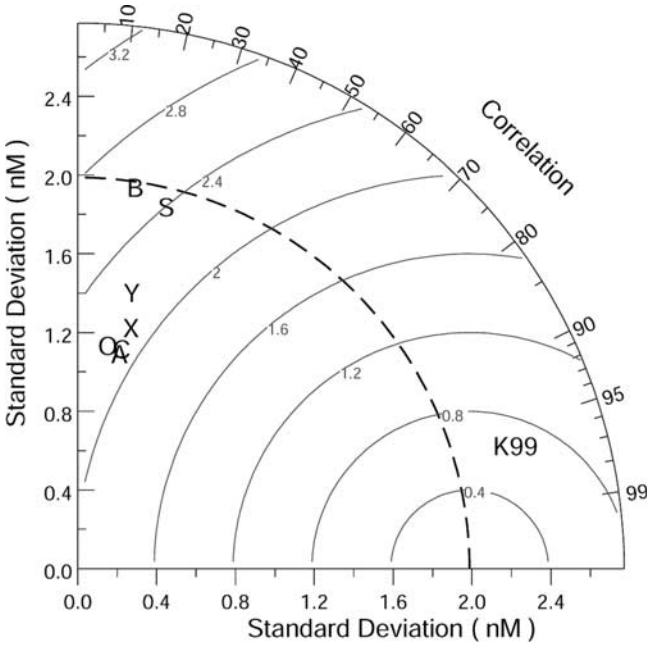

Figure 1. Pattern statistics describing the total space-time variations of DMS concentration as obtained from six gridded climatologies compared with that of *Kettle and Andreae* [2000]. Mean (X) and median (Y) values of the climatologies A, O, S, C, and B are also reported. To read this Taylor diagram, a polar plot, one compares the standard deviation of each spatiotemporal field (the radius corresponding to each label) to the standard deviation of the reference climatology of *Kettle and Andreae* [2000]. For instance, if a field exhibits less overall variance than the reference, the corresponding distance between the origin and the label will be less than the dashed curve which crosses the X-axis at the reference point. The other axis, the angular coordinate indicates the correlation coefficient r between a given climatology and the reference. The distance from the reference point to any label is the central pattern RMS difference.

of the *r* axis on Figure 1. As expected, there is a high correlation between the *Kettle et al.* [1999] and the *Kettle and Andreae* [2000] climatologies. The latter is an update with about 10% more DMS measurements than the former. Unfortunately, the *r*s of all other climatologies, relative to the reference, are less than 0.25. Thus their variability is colocated with at most only 6% of the variability of the reference ($r^2 < 0.06$). Another commonly used statistic (not shown in Figure 1) is the overall bias, i.e., the area-weighted, global annual mean for a given climatology minus that of the reference. The smallest overall bias comes from the mean climatology X (-0.04 nmol L^{-1}), i.e., the average of all climatologies, except the reference and K99, for each grid point. The bias for the median climatology Y is also small (-0.13 nmol L^{-1}) relative to those from most of the individual climatologies (0.12 for K99, 0.54 for A, -0.31 for O, 0.26 for S, -0.51 for C, and -0.42 for B).

[7] These large differences in overall variability motivated further analysis of mean spatial and temporal variability. We found large differences among global maps of annual mean DMS concentrations (Figure 2). The annual mean DMS field from *Anderson et al.* [2001] has almost no spatial variability. Similarly, the *Belviso et al.* [2004] climatology has little spatial variability in most of the low-DMS areas, except for the tropical South Pacific. However, the minimum DMS concentrations of *Belviso et al.* [2004] are roughly half those of *Anderson et al.* [2001]. DMS levels are lowest of all in the tropical gyres of the *Chu et al.* [2003] climatology. There is no clear tendency for the equatorial Pacific and the adjacent Inter-Tropical Convergence Zone: Some of the climatologies have enhanced DMS concentrations [*Kettle and Andreae*, 2000; *Chu et al.*, 2003; *Aumont et al.*, 2002; *Simó and Dachs*, 2002], whereas the others do not [*Anderson et al.*, 2001; *Belviso et al.*, 2004]. The Anderson et al. and Belviso et al. approaches both produce DMS highs in subtropical and frontal systems between 40°S and 50°S. In the Southern Ocean between 40°S and 60°S, the *Simó and Dachs* [2002] climatology predicts low annual mean concentrations, due to strong winds and deep mixed layers. Much higher concentrations are predicted by the other climatologies, but only Kettle estimates very high DMS concentrations in the biogeochemical province that is adjacent to Antarctica. In the Atlantic north of 40°N, *Simó and Dachs* [2002] predict the lowest annual mean concentrations, probably because of the weight they give to deep mixed layers in winter and spring.

[8] To study seasonal variability, we also compared the annual cycle of zonal mean surface DMS concentrations using latitude-time (Hövmöller) plots (Figure 3). DMS patterns of *Simó and Dachs*'s [2002] and *Kettle and Andreae*'s [2000] climatologies are similar, although high-latitude summer concentrations are much larger in the latter. The *Belviso et al.* [2004] and *Anderson et al.* [2001] climatologies also exhibit high DMS north of 50°N, but they are more persistent. Furthermore, in the latter, there is remarkably little latitudinal and seasonal variability between 40°S and 50°N. There is also little seasonal variability between 40°S and 40°N in the climatologies from *Belviso et al.* [2004], *Aumont et al.* [2002], and *Chu et al.* [2003]. Unlike the former climatology, the latter two climatologies do show substantial latitudinal variability in this 40°S to 40°N region.

[9] Directly comparing gridded climatologies has allowed us to compare maps and zonal means, as well as a Taylor diagram weighted by area, but it is also important to compare the climatologies to discrete measurements of sea-surface DMS. Thus, with the existing database of discrete DMS measurements (available at http://saga.pmel.noaa.gov/dms/), we subsampled the climatologies at the same positions and months. Then we made a Taylor diagram where all discrete measurements are weighted equally (Figure 4). This diagram reveals only extremely weak correlations with the observations and every climatology, even those that use the identical database of measurements to develop their algorithms [*Kettle and Andreae*, 2000; *Anderson et al.*, 2001; *Simó and Dachs*, 2002]. The overall bias between the observations and the subsampled climatologies are -0.33, -0.36, 0.16, -1.38, 0.44, -1.47,

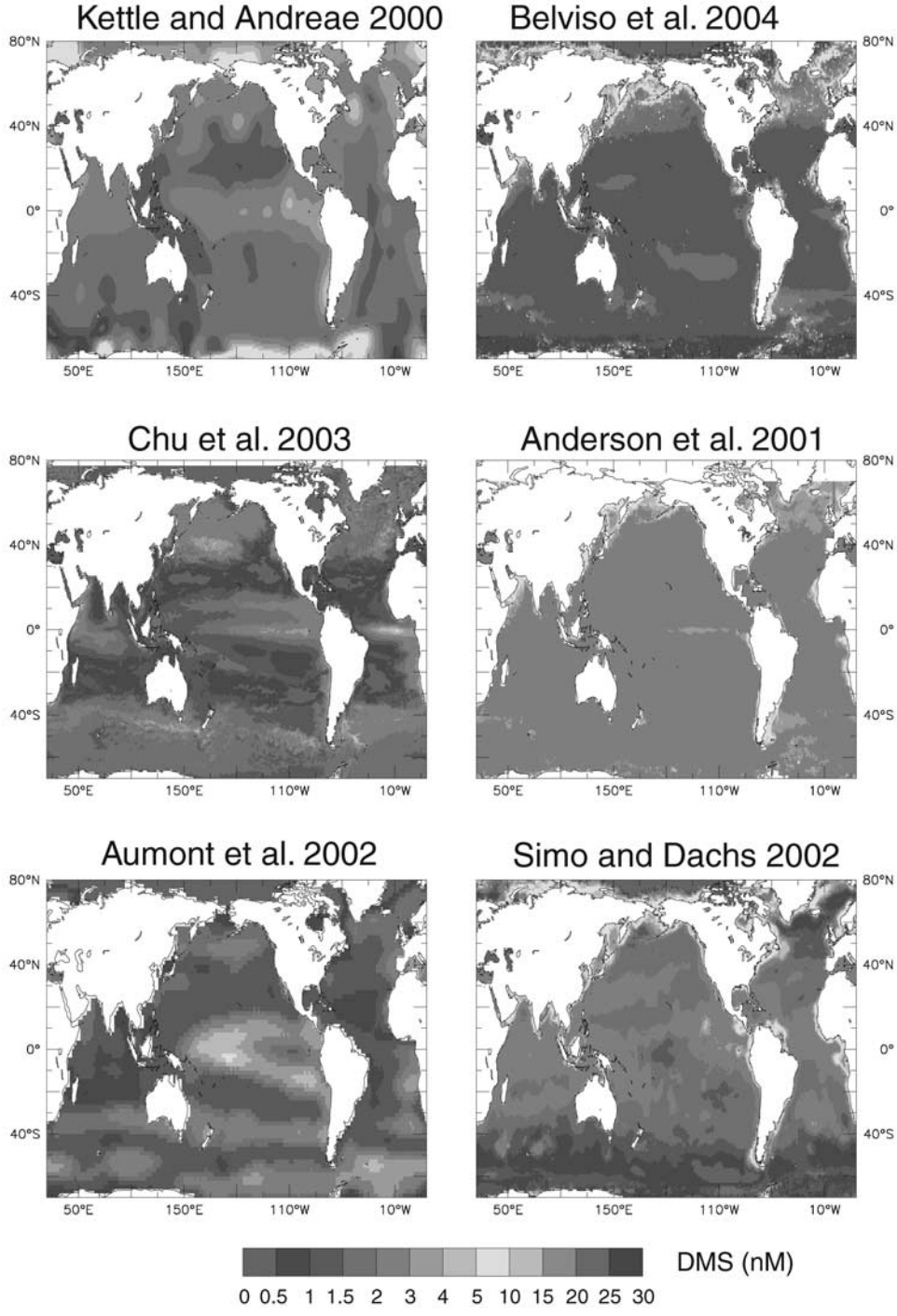

Figure 2. Global maps of the annual mean surface concentration of DMS in nmol L^{-1}. See color version of this figure at back of this issue.

0.30, −0.42, or −0.71 nmol L^{-1} for K, K99, A, O, S, C, B, mean (X), and median (Y), respectively (data not shown). The overall bias for *Anderson et al.* [2001] is lowest. Conversely, the bias is largest for *Chu et al.* [2003], which is closely followed by *Aumont et al.* [2002].

[10] New DMS measurements [*Belviso et al.*, 2004] carried out during the French Programme Océan Multidisciplinaire Méso Echelle (POMME) project (http://www.lodyc.jussieu.fr/POMME/) provide an independent test; that is, they are not part of the discrete DMS measurement database that was used to develop the parameterizations to construct the climatologies. For the POMME area (38°N–45°N, 16.5°W–21°W), located midway between the Portuguese coast and the Azores, the *Kettle and Andreae* [2000] database contains only 20 DMS measurements (samples were collected between April 1987 and

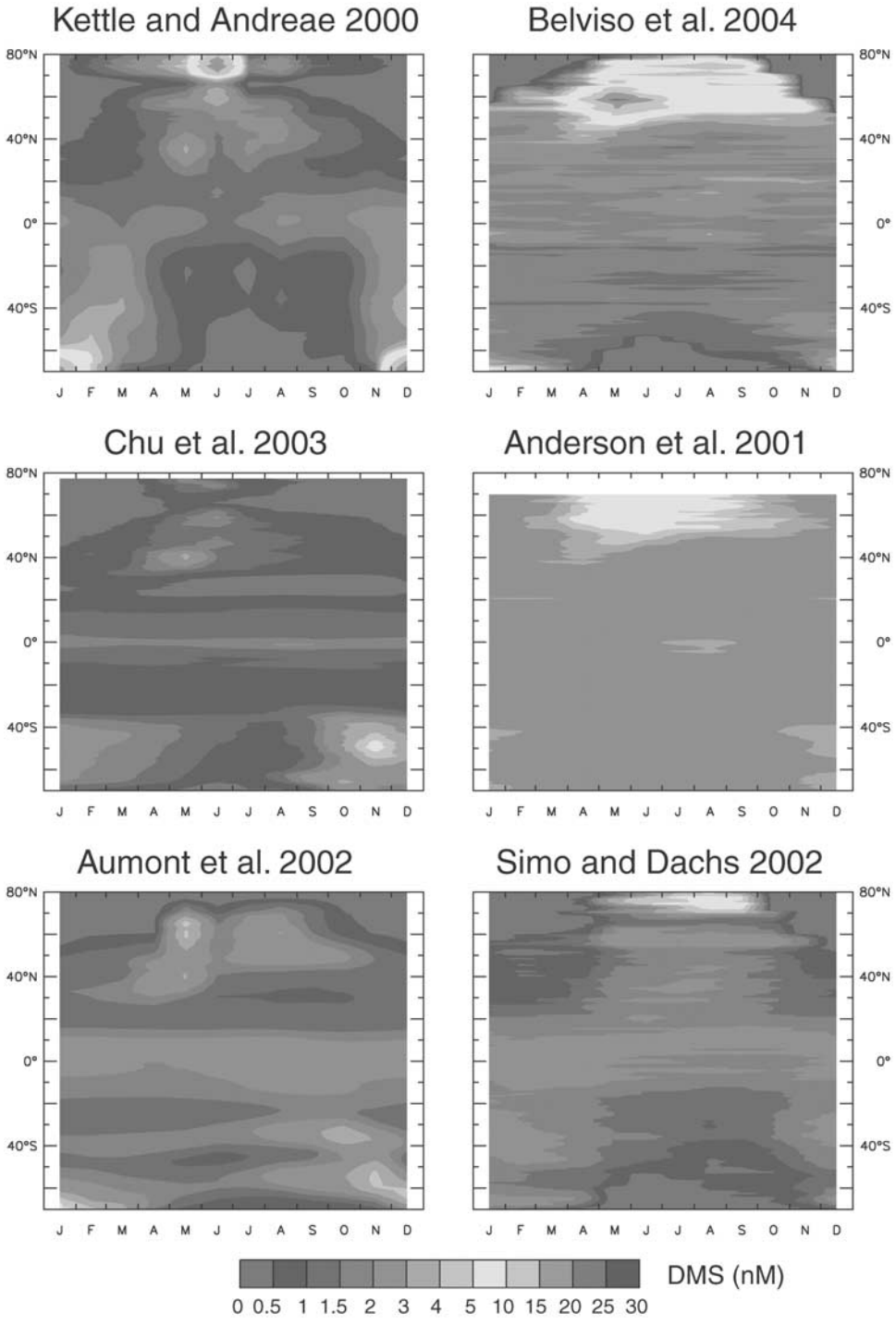

Figure 3. Latitude-time plots of the sea-surface concentration of DMS. See color version of this figure at back of this issue.

May 1993). Conversely, during the three POMME cruises in late winter (POMME I), spring (POMME II), and late summer 2001 (POMME III), there were 225 new measurements of sea-surface DMS measurements. Figure 5 shows the observed distribution of these new surface DMS measurements versus results from the different climatologies. The climatologies of *Anderson et al.* [2001] and *Belviso et al.* [2004] markedly overestimate DMS in winter (POMME 1) throughout the area, and in spring (POMME 2) north of 42°N. Conversely, DMS levels predicted by *Chu et al.* [2003] provide the best match with the data during winter and spring; however, they overestimate the data in summer. Better agreement in summer comes from the *Belviso et al.* [2004] climatology throughout the domain

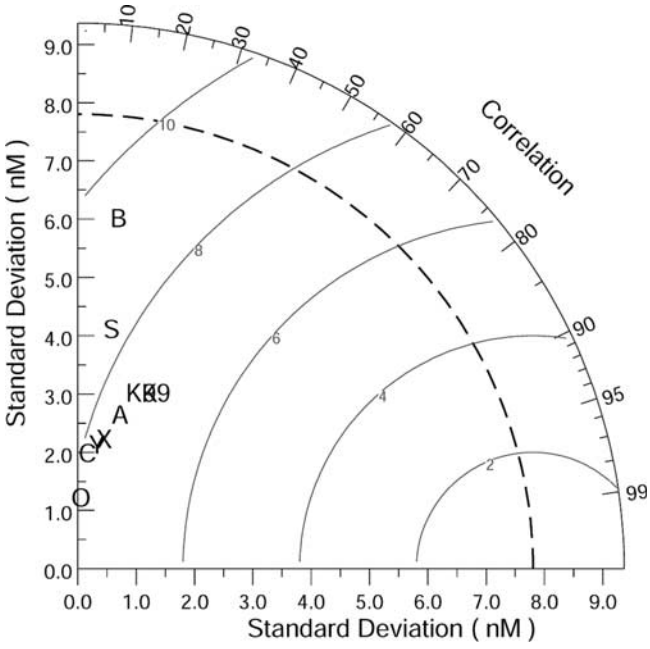

Figure 4. Taylor diagram for sea-surface DMS showing summary statistics for the different climatologies and the DMS data. Kettle's files that we used are those with no data-assimilation correction. Also shown are the mean (X) and median (Y) values of the climatologies A, O, S, C, and B.

and from *Aumont et al.* [2002] climatology south of 42°N. Predictions from *Simó and Dachs* [2002] agree with the winter observations south of 42°N. To gain insight into the methodology of Simó and Dachs, DMS was recalculated using the POMME chlorophyll *a* measurements (H. Claustre, Laboratoire d'Océanographie de Villefranche-sur-mer, personal communication, 2002) and mixed layer depth (MLD) from the POMME measurements of temperature and salinity (G. Caniaux, Meteo-France, personal communication, 2004). The definition for MLD is identical (depth where $\Delta\sigma_t = 0.125$ kg m^{-3} relative to the surface). When applied to the in situ observations of MLD and Chl *a*, algorithm (2) of *Simó and Dachs* [2002] (for Chl a/MLD > = 0.02) underestimates DMS levels in the POMME area (Figure 6a). However, the highest Chl-to-MLD ratio during POMME was 0.062, which is rather low relative to the ratios used by *Simó and Dachs* [2002]. When applied to the in situ observations of MLD, algorithm (1) of *Simó and Dachs* [2002] (for Chl a/MLD < 0.02) overestimates DMS levels in the POMME area when the MLD < 50 m (i.e., all during cruise POMME 3); conversely, it generally underestimates DMS levels during the winter and early spring periods where MLD > 50 m (Figure 6b). Another difference is that during POMME, the MLD was often found to be deeper than 110 m, whereas algorithm (1) of *Simó and Dachs* [2002] is based on shallower MLDs. Thus the algorithms of *Simó and Dachs* [2002] are less adapted for the northeast Atlantic than for the Sargasso Sea. Indeed, in the Sargasso Sea at the Bermuda Atlantic Time Series station (BATS), the *Simó and Dachs* [2002] climatology provides a good match to the observed timing and amplitude of the annual cycle in sea surface DMS [see *Simó and Dachs*, 2002, Figure 3]. At BATS, the other climatologies, except *Anderson et al.* [2001], show some agreement with observations in winter and spring, but they fail to reproduce the observed DMS enhancement in summer.

[11] Following the lead of *Bopp et al.* [2003], we also compared DMS fields to surface DMS measurements along seven ship tracks from different ocean regions (Figure 7). The *Kettle and Andreae* [2002] climatology generally

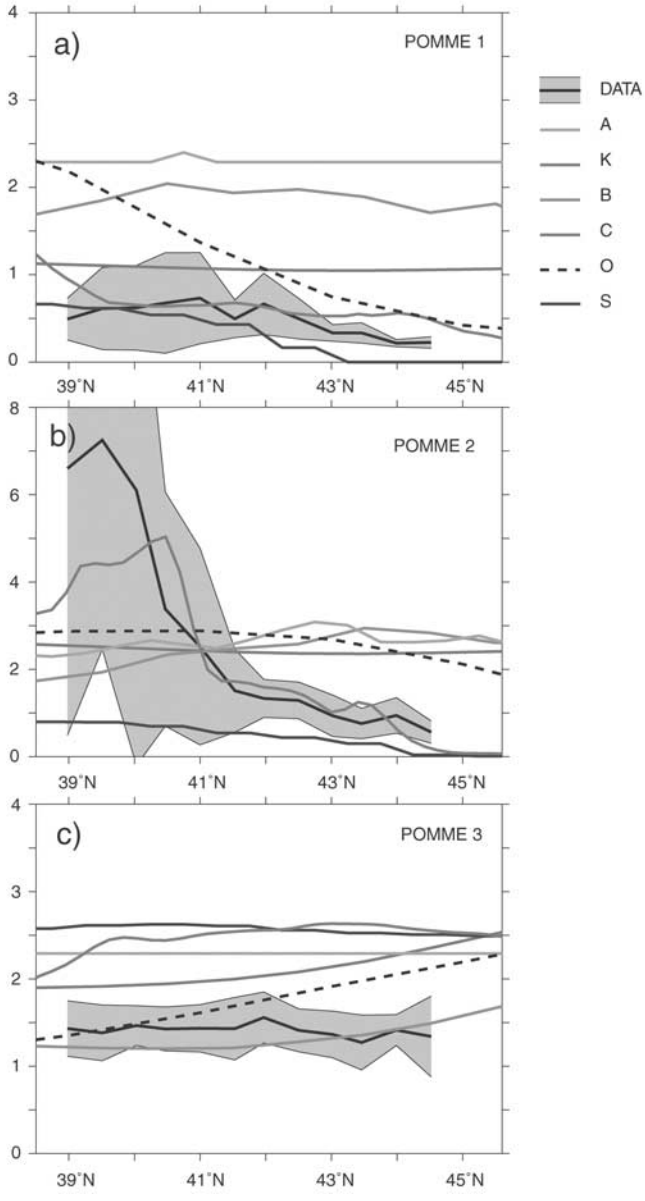

Figure 5. Latitudinal variability in the POMME area for observed DMS concentration, plotted as the mean (solid black line) and range (shaded area) of the discrete measurements carried out every $^1/_2$ degree of latitude, versus zonal means for 16°W–21°W from the different climatologies during (a) February 2001, (b) March–April 2001, and (c) August–September 2001. See color version of this figure at back of this issue.

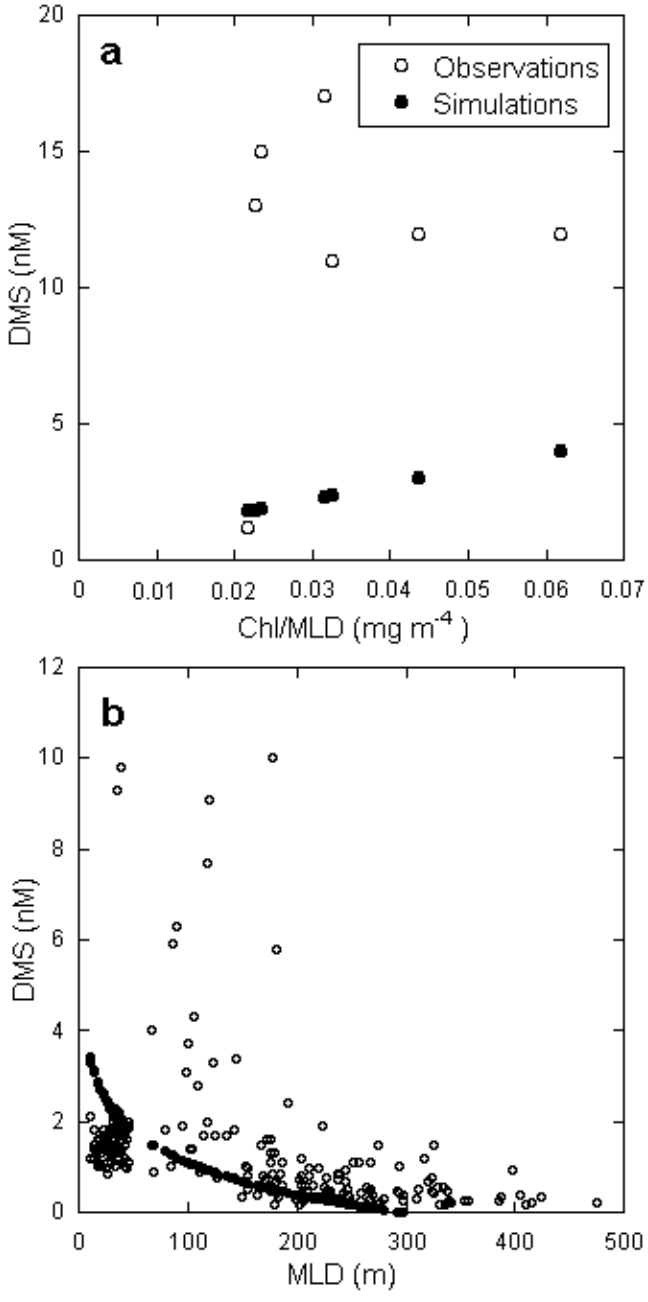

Figure 6. Evaluation of the double algorithm of *Simó and Dachs* [2002] (a) for Chl/MLD equal or higher than 0.02, and (b) for Chl/MLD lower than 0.02. Shown in black dots are the DMS levels predicted by the algorithms of *Simó and Dachs* [2002] using local MLDs. In *Simó and Dachs* [2002], only data pairs with a Chl/MLD equal or higher than 0.02 were correlated linearly with DMS (algorithm (2) of *Simó and Dachs* [2002]) as the black dots in Figure 6a show. For Chl/MLD lower than 0.02, Simó and Dachs found a logarithmic negative correlation between DMS and MLD with no contribution from Chl. (algorithm (1) of *Simó and Dachs* [2002]), as the black dots in Figure 6b show.

matches the observations. This is expected because these same data are part of the *Kettle et al.* [1999] database and they are thus assimilated to provide the climatological estimates. In the Atlantic (Figures 7a and 7b), none of the climatologies has sufficient resolution to reproduce the observed mesoscale variability. However, the correct order of magnitude of spatial variations of the observed DMS in the Atlantic is generally captured by *Aumont et al.* [2002]. Although *Aumont et al.* [2002] used the field observations of Figure 7a to develop their algorithms, an independent test of their approach is offered by the tropical Atlantic data (Figure 7b). The prognostic model results from *Chu et al.* [2003] show about the right spatial variability between the equator and 30°N (Figure 7a), but in the South Atlantic subtropical gyre (Figures 7a and 7b), estimated DMS is much too low. In the North Pacific, all climatologies fail to reproduce the high DMS levels observed between 150°W and 170°W (Figure 7c). The same tendency is found in the Southern Ocean at 52°E between 33°S and 43°S (Figure 7g). In the equatorial Pacific, there is rather good agreement between observations and the fields from *Simó and Dachs* [2002], *Chu et al.* [2003], and *Anderson et al.* [2001] (Figures 7d and 7e). In the Southern Ocean at 145°E, the climatology from *Belviso et al.* [2004] is most realistic, whereas the *Chu et al.* [2003] climatology considerably overestimates DMS (Figure 7f).

4. Discussion

[12] A large source of uncertainty in studies of the global sulfur cycle lies in estimating the flux of DMS from the oceans to the atmosphere and the fate of DMS in the atmosphere. Reducing these uncertainties is vital to improving our understanding of the role of DMS in climatic feedbacks. The sea-to-air DMS flux has been formulated simply as the product of the sea surface concentration and the gas transfer rate of DMS. Uncertainties in the gas transfer rates have been evaluated by *Nightingale et al.* [2000]. Although the seven published DMS climatologies exhibit large differences in the spatiotemporal distribution of sea-surface DMS (Figures 1, 2, and 3), north of 50°N the climatologies agree at least that there is strong seasonal variation of DMS. However, even in that region, the seasonal amplitude differs markedly (Figure 3). At lower latitudes (20°–40°) the climatologies disagree as to whether there is substantial variability in sea-surface DMS; the multiyear time series stations at BATS (32°N) and Amsterdam Island (37°S) stations clearly show large variability [*Dacey et al.*, 1998; *Putaud et al.*, 1992]. There is also disagreement between 40°S and 60°S, for both the seasonal amplitude and the summer maximum. In that zone, high wind speeds result in high gas exchange coefficients [*Nightingale et al.*, 2000]. When these large coefficients are combined with moderate-to-high summer DMS concentrations, as predicted by *Kettle and Andreae* [2000] and *Chu et al.* [2003], this yields very high DMS emissions. To assure its representativity, it is crucial for the sparse data set in that zone to be complemented by new measurements. Moreover, that same zone is also where the largest changes in DMS emissions are expected under global warming [*Bopp et al.*, 2003].

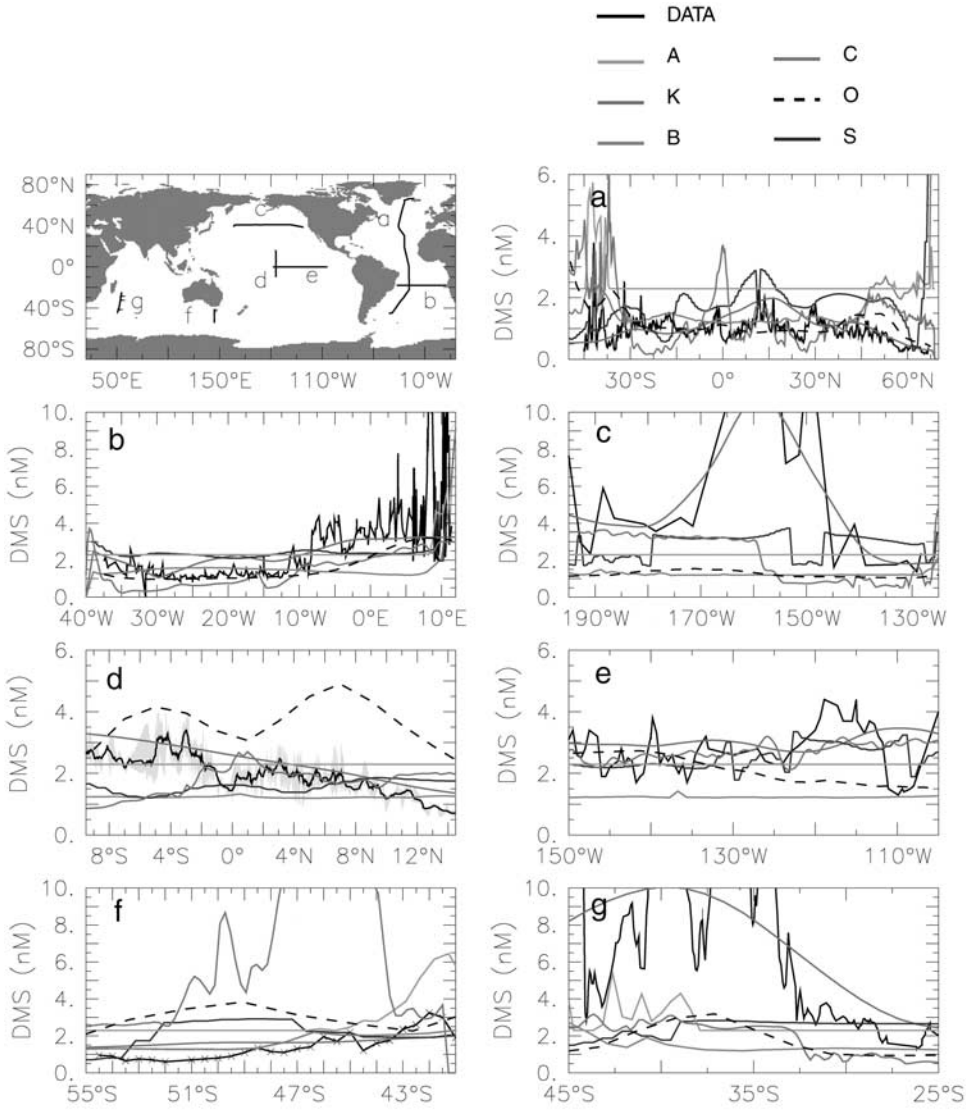

Figure 7. Variations of surface DMS (nmol L^{-1}) along different cruise tracks. See color version of this figure at back of this issue.

[13] Seasonal variations of DMS simulated by *Simó and Dachs* [2002] are in much better agreement with observations at BATS than in the POMME area. Assuming August is representative of summer, climatological MLDs are slightly higher in the POMME area (mostly between 20 and 30 m) than at BATS (10–20 m). This results in simulated DMS levels in the POMME region of 2.5 nmol L^{-1} (Figure 5c) that are slightly lower than those of 3 nmol L^{-1} at BATS [*Simó and Dachs*, 2002, Figure 3]. Observed MLDs in the POMME area ranged from 10 to 45 m (30.8 ± 8.8 m (±1σ), n = 83), and were thus slightly higher than the MLDs estimated by the climatology. Thus part of the difference in observed and climatological DMS estimates for POMME 3 (Figure 5c) result from differences in reconstructed and observed MLDs. Relative to observations in February, climatological winter MLDs are typically much deeper in the POMME area (140–240 m) than at BATS (140–160 m). Hence the POMME region's simulated DMS concentrations of 0–0.7 nmol L^{-1} are lower than those of at BATS (1 nmol L^{-1}), [*Simó and Dachs*, 2002]. Measured MLDs in the POMME region (260 ± 66 m) are deeper than the climatological estimates. Thus the discrepancy between the observed and climatological estimates of DMS during POMME 1 north of 42°N (Figure 5a) cannot result from differences in climatological and observed MLDs. Instead, the algorithm itself must not be adapted to predict DMS levels when MLDs are deeper than 200–300 m. The same probably also holds for POMME 2 north of 42°N where measured MLDs are also too deep (200 ± 90 m) for the climatological algorithm. The opposite tendency is found in some of the southern areas of the POMME region, i.e., south of 42°N, where observed MLDs range from 10 to 30 m. In those southern areas, the very large discrepancies between observed and climatological estimates of DMS (Figure 5b) partly results from the climatological MLDs being too deep. In summary, errors

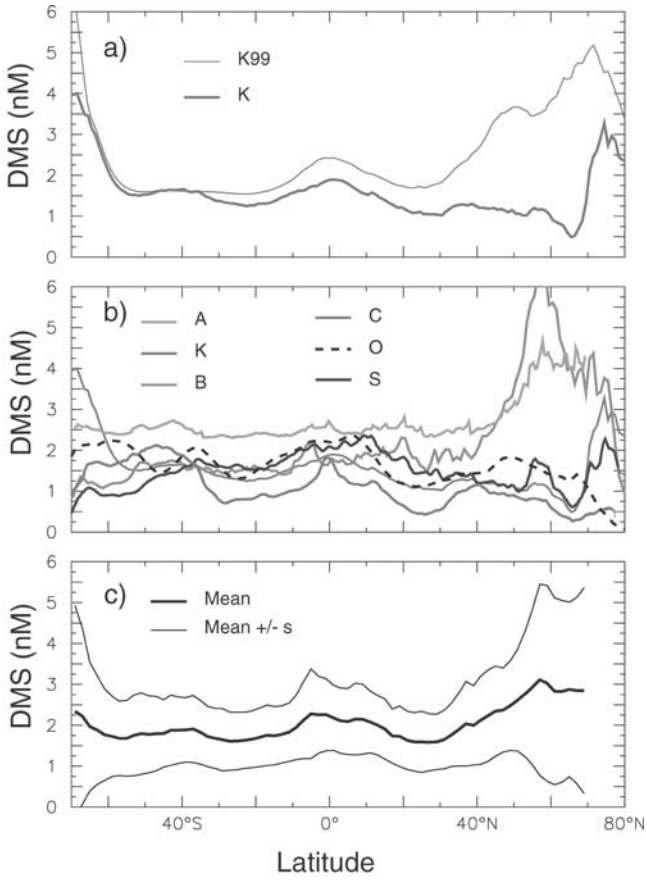

Figure 8. Summary of climatological zonal annual means of sea surface DMS: (a) Sensitivity of the climatology of *Kettle et al.* [1999] to data updating. (b) Intercomparison of the six climatologies. (c) Mean $\pm 1\sigma$ for the six climatologies. See color version of this figure at back of this issue.

in climatological MLD only partly explain seasonal differences between the observed and climatological DMS estimates from *Simó and Dachs* [2002]. Their climatological algorithms are not robust when climatological MLDs are deeper than 200–300 m. The limits of their approach for predicting in situ instantaneous DMS concentrations are further revealed by a logarithmic regression with the POMME data set when Chl/MLD < 0.02, which only explains 9% of the variance (Figure 6b).

[14] Differences in the zonal annual means of the various climatologies are shown in Figure 8. The large sensitivity of the *Kettle et al.* [1999] methodology to the number of DMS measurements, particularly in the Northern Hemisphere, suggests that at least for that region it may be too early to produce an accurate DMS climatology from existing measurements. In the tropics, there is less divergence among estimates (Figure 8b), but even there, agreement as represented by the range/mean is rarely lower than 50% (Figure 8c). Agreement worsens to nearly 100% at high latitudes.

[15] The seven climatologies have different advantages and disadvantages as revealed by their ability to match observed distributions of sea-surface DMS in selected oceanic regions. The best data coverage is offered by the Atlantic and equatorial Pacific (http://saga.pmel.noaa.gov/dms/). The fields of *Aumont et al.* [2002] offer better agreement with the observed DMS distribution in the Atlantic Ocean north of 40°S. In contrast, in the same region the *Anderson et al.* [2001] and *Belviso et al.* [2000] winter maps (Figures 3 and 5) markedly overestimate DMS in the high latitudes. Moreover, the climatology of Aumont et al. also exhibits seasonal variations in the North Atlantic in general agreement with observations. Furthermore, Aumont et al.'s background concentrations of DMS in the Atlantic subtropical gyres show the best agreement with those observed, whereas those from *Chu et al.* [2003] are too low (Figures 7a and 7b). Only Aumont et al.'s provides an independent evaluation of the community structure of marine phytoplankton (as a prognostic model variable). In the approach taken by *Belviso et al.* [2004], DMS relies too much on chlorophyll because the community structure index is diagnosed from chlorophyll concentrations. The *Simó and Dachs* [2002] DMS climatology relies too much on the climatological MLDs and yields very low DMS levels north of 40°N up to late April, at the onset of the spring phytoplankton bloom. It remains a challenge for the community to establish a better algorithm of DMS production with an improved description of effects due to the MLD, phytoplankton biomass, and the community structure.

[16] Our recommendation for those studying the atmospheric DMS cycle over the Pacific Ocean would be to use either the climatology of *Simó and Dachs* [2002] or that from *Chu et al.* [2003], because both accurately track the observations in the equatorial Pacific. The *Anderson et al.* [2001] climatology also provides the right order for annual mean concentrations, but it does not resolve the variations in sea-surface DMS concentration. Anderson et al. state that the simplicity of their algorithm makes it suitable for use in global studies, although it may not capture local variability in DMS. Unfortunately, none of these climatologies adequately resolve the highs in DMS found in the North Pacific (Figure 7c).

[17] For studies concerning the sulfur cycle and the Southern Ocean, our limited evaluation suggests using DMS fields based on SeaWiFS imagery. Yet one such climatology, from *Anderson et al.* [2001], estimates excessive winter background DMS concentrations (2.3 nmol L^{-1}) in ice-free areas. Conversely, the winter DMS fields from *Belviso et al.* [2004] and *Simó and Dachs* [2002] do not have this problem. Still though, *Simó and Dachs* [2002] probably underestimate winter and springtime DMS because Southern Ocean mixed layer depths are often deeper than 200–300 m. Furthermore, *Belviso et al.* [2004] DMS climatology appears too tightly linked to the fields of chlorophyll.

5. Conclusion

[18] The comparison of seven different DMS climatologies has provided a first estimate of the uncertainty in quantifying the global distribution of sea-surface DMS. For the zonal and annual mean, uncertainties range from 50% in the tropics to 100% in the high latitudes. Uncer-

tainties in sea-surface DMS concentrations are even larger than those associated with the gas transfer coefficient, which are approximately 50% according to *Nightingale et al.* [2000]. Thus the DMS flux is not known to within even a factor of 2. Regional evaluation of the different climatologies provides an indication as to which ones are best suited for use with regional atmospheric sulfur models. The *Aumont et al.* [2002] climatology is best suited for the Atlantic Ocean, whereas of the climatologies from *Simó and Dachs* [2002] and *Chu et al.* [2003] are preferable for the equatorial Pacific zone. The *Belviso et al.* [2004] climatology appears best suited for the Southern Ocean. The fields of *Anderson et al.* [2001] reproduce the global annual mean DMS and DMS highs in the high latitudes; however, they fail to resolve variability in the low-DMS areas over most of the rest of the ocean. The pioneering modeling work of *Chu et al.* [2003], which includes basic prognostic formulations of DMS production and removal processes, should be pursued; improved formulations should also account for sources and sinks of dimethylsulfoniopropionate (DMSP), the major precursor of DMS. Evaluation of new model formulations will benefit from the rapidly growing database of marine DMSP.

[19] **Acknowledgments.** We thank Jean-Marie Epitalon and Charles Doutriaux for technical assistance in making Taylor diagrams. We also thank G. Caniaux (Meteo-France) and H. Claustre (LOV) for MLD and pigment data. Finally, we thank I. Lefevre and C. Valant who contributed to DMSP/DMS analyses during the POMME expeditions. This work was supported by the national program PROOF of INSU/CNRS. The contribution from R. Simó was funded by the Spanish Ministry of Science and Technology through the AMIGOS project (REN2001-3562CLI). This is LSCE contribution 1110.

References

Anderson, T. R., S. A. Spall, A. Yool, P. Cipollini, P. G. Challenor, and M. J. R. Fasham (2001), Global fields of sea surface dimethylsulfide predicted from chlorophyll, nutrients and light, *J. Mar. Syst.*, *30*, 1–20.

Andreae, M. O. (1990), Ocean-atmosphere interactions in the global biogeochemical sulfur cycle, *Mar. Chem.*, *30*, 1–29.

Aumont, O., S. Belviso, and P. Monfray (2002), Dimethylsulfoniopropionate (DMSP) and dimethylsulfide (DMS) sea surface distributions simulated from a global three-dimensional ocean carbon cycle model, *J. Geophys. Res.*, *107*(C4), 3029, doi:10.1029/1999JC000111.

Ayers, G. P., and R. W. Gillett (2000), DMS and its oxidation products in the remote marine atmosphere: Implications for climate and atmospheric chemistry, *J. Sea Res.*, *43*, 275–286.

Bates, T. S., J. D. Cline, R. H. Gammon, and S. R. Kelly-Hansen (1987), Regional and seasonal variations in the flux of oceanic dimethylsulfide to the atmosphere, *J. Geophys. Res.*, *92*, 2930–2938.

Belviso, S., O. Aumont, L. Bopp, F.-M. Breon, P. Couvert, and P. Monfray (2000), Assessment of the marine biota-DMS-cloud-climate hypothesis using remotely sensed data and an ocean general circulation model (OGCM), in *Remote Sensing of the Ocean and Sea Ice 2000*, edited by C. R. Bostater Jr. and R. Santoreli, *Proc. SPIE Int. Soc. Opt. Eng.*, *4172*, 102–110.

Belviso, S., C. Moulin, L. Bopp, and J. Stefels (2004), Assessment of a global climatology of oceanic dimethylsulfide (DMS) concentrations based on SeaWiFS imagery (1998–2001), *Can. J. Fish. Aquat. Sci.*, *61*(5), 804–816.

Bopp, L., O. Aumont, S. Belviso, and P. Monfray (2003), Potential impact of climate change on marine dimethylsulfide emissions, *Tellus, Ser. B*, *55*, 11–22.

Bopp, L., O. Boucher, O. Aumont, S. Belviso, J.-L. Dufresne, M. Pham, and P. Monfray (2004), Will marine dimethylsulfide emissions amplify or alleviate global warming?—A model study, *Can. J. Fish. Aquat. Sci.*, *61*(5), 826–835.

Boucher, O., et al. (2003), DMS atmospheric concentrations and sulphate aerosol indirect radiative forcing: A sensitivity study to the DMS source representation and oxidation, *Atmos. Chem. Phys.*, *3*, 49–65.

Charlson, R. J., J. E. Lovelock, M. O. Andreae, and S. G. Warren (1987), Oceanic phytoplankton, atmospheric sulphur, cloud albedo and climate, *Nature*, *326*, 655–661.

Chu, S., S. Elliott, and M. E. Maltrud (2003), Global eddy permitting simulations of surface ocean nitrogen, iron, sulfur cycling, *Chemosphere*, *50*, 223–235.

Dacey, J. W. H., F. A. Howse, A. F. Michaels, and S. G. Wakeham (1998), Temporal variability of dimethylsulfide and dimethylsulfoniopropionate in the Sargasso Sea, *Deep Sea Res., Part I*, *45*, 2085–2104.

Erickson, D. J., III, S. J. Ghan, and J. E. Penner (1990), Global ocean-to-atmosphere dimethylsulfide flux, *J. Geophys. Res.*, *95*, 7543–7552.

Esbensen, S. K., and Y. Kushnir (1981), The heat budget of the global ocean: An atlas based on estimates from marine observations, *Rep. 19*, Clim. Res. Inst., Oreg. State Univ., Corvallis.

Gabric, A. J., P. H. Whetton, and R. Cropp (2001), Dimethylsulphide production in the subantarctic Southern Ocean under enhanced greenhouse conditions, *Tellus, Ser. B*, *53*, 273–287.

Jones, A., D. L. Roberts, M. J. Woodage, and C. E. Johnson (2001), Indirect sulphate aerosol forcing in a climate model with an interactive sulphur cycle, *J. Geophys. Res.*, *106*, 20,293–20,310.

Kettle, A. J., and M. O. Andreae (2000), Flux of dimethylsulfide from the oceans: A comparison of updated data sets and flux models, *J. Geophys. Res.*, *106*, 26,793–26,808.

Kettle, A. J., et al. (1999), A global database of sea surface dimethylsulfide (DMS) measurements and a procedure to predict sea surface DMS as a function of latitude, longitude, and month, *Global Biogeochem. Cycles*, *13*, 399–444.

Nightingale, P. D., G. Malin, C. S. Law, A. J. Watson, P. S. Liss, M. I. Liddicoat, J. Boutin, and R. C. Upstill-Goddard (2000), In situ evaluation of air-sea exchange parameterizations using novel conservative and volatile tracers, *Global Biogeochem. Cycles*, *14*, 373–387.

Putaud, J. P., N. Mihalopoulos, B. C. Nguyen, J. M. Campin, and S. Belviso (1992), Seasonal variations of atmospheric sulfur dioxide and dimethylsulfide concentrations at Amsterdam Island in the Southern Indian Ocean, *J. Atmos. Chem.*, *15*, 117–131.

Shaw, G. E. (1983), Bio-controlled thermostasis involving the sulfur cycle, *Clim. Change*, *5*, 297–303.

Simó, R., and J. Dachs (2002), Global ocean emission of dimethylsulfide predicted from biogeophysical data, *Global Biogeochem. Cycles*, *16*(4), 1018, doi:10.1029/2001GB001829.

Taylor, K. E. (2001), Summarizing multiple aspects of model performance in a single diagram, *J. Geophys. Res.*, *106*, 7183–7192.

T. R. Anderson, Southampton Oceanography Center, Waterfront campus, University of Southampton, European Way, Southampton SO14 3ZH, UK. (tra@soc.soton.ac.uk)

O. Aumont, Laboratoire d'Océanographie Dynamique et de Climatologie, Université Pierre et Marie Curie, 4 Place Jussieu, 75252 Paris Cedex 5, France. (aumont@lodyc.jussieu.fr)

S. Belviso, L. Bopp, C. Moulin, and J. C. Orr, Laboratoire des Sciences du Climat et de l'Environnement, UMR CEA-CNRS 1572 & IPSL, CEN-Saclay, Bât 701 L'Orme des Merisiers, 91191 Gif-sur-Yvette, France. (belviso@lsce.saclay.cea.fr; bopp@lsce.saclay.cea.fr; moulin@lsce.saclay.cea.fr; orr@lsce.saclay.cea.fr)

S. Chu, S. Elliott, and M. E. Maltrud, Climate, Ocean and Sea Ice Modeling Project (COSIM), Los Alamos National Laboratory, Los Alamos, NM 87545, USA. (spchu@lanl.gov; sme@lanl.gov; maltrud@lanl.gov)

R. Simó, Institut de Ciències del Mar (CMIMA-CSIC), Pg Maritim de la Barceloneta 37-49, 08003 Barcelona, Spain. (rsimo@icm.csic.es)

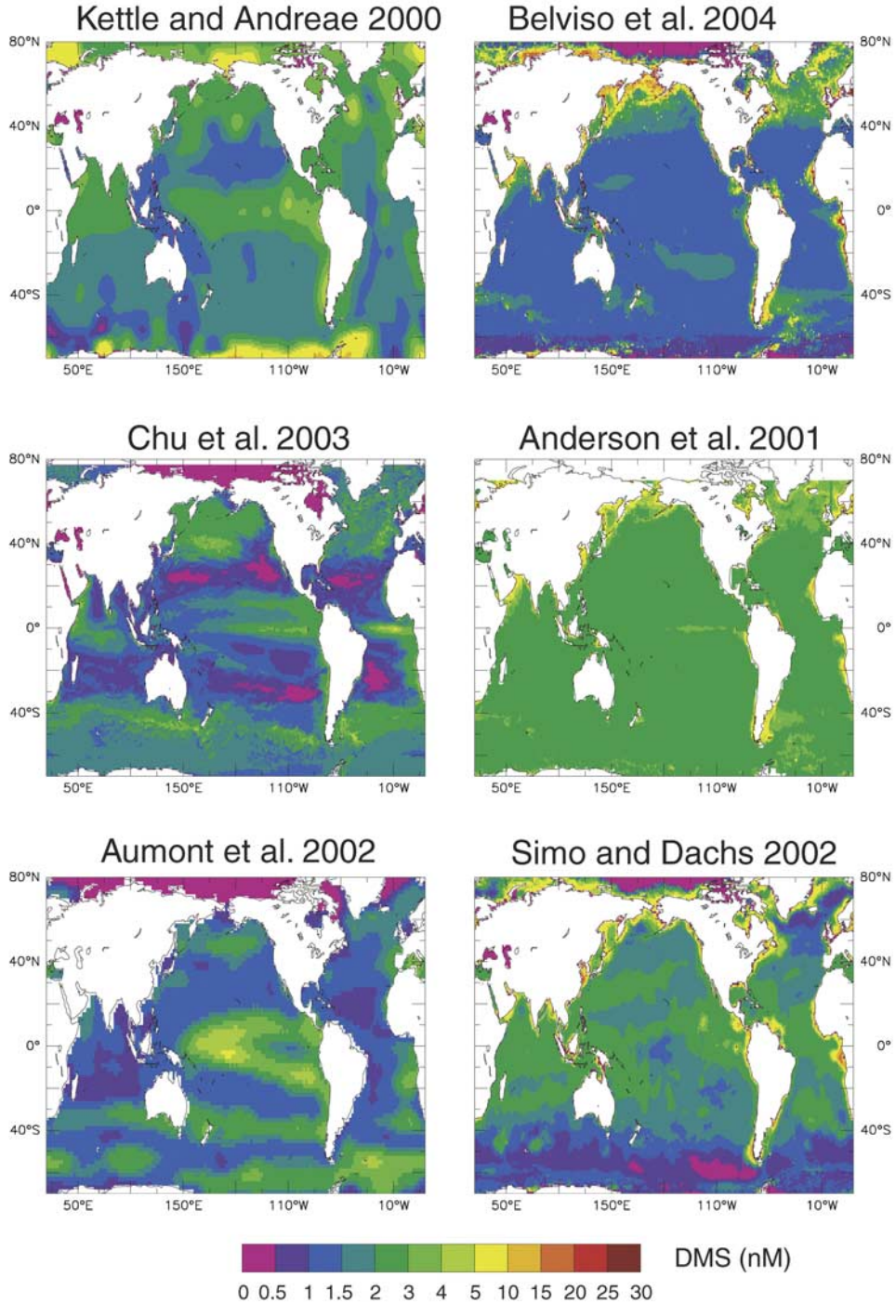

Figure 2. Global maps of the annual mean surface concentration of DMS in nmol L^{-1}.

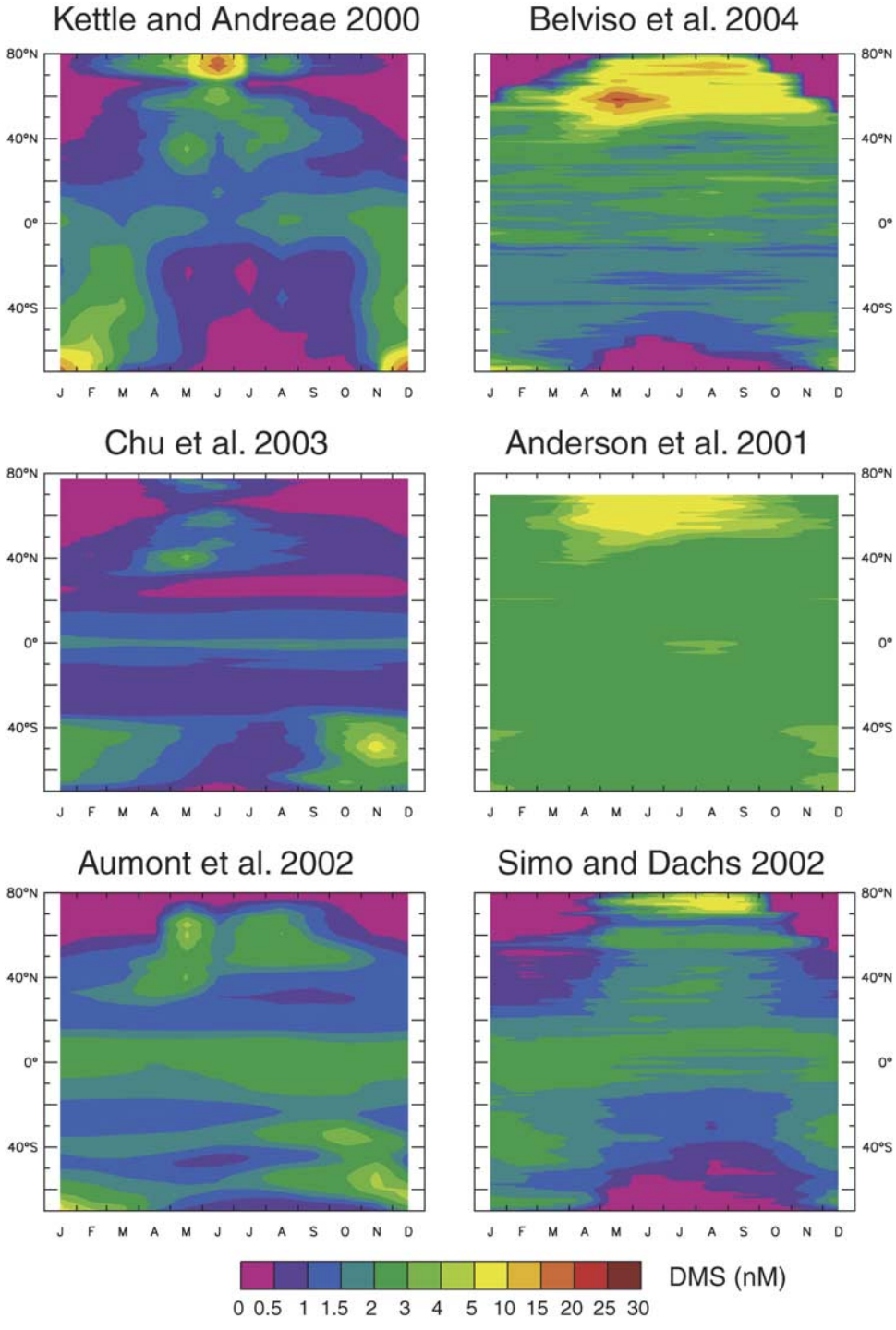

Figure 3. Latitude-time plots of the sea-surface concentration of DMS.

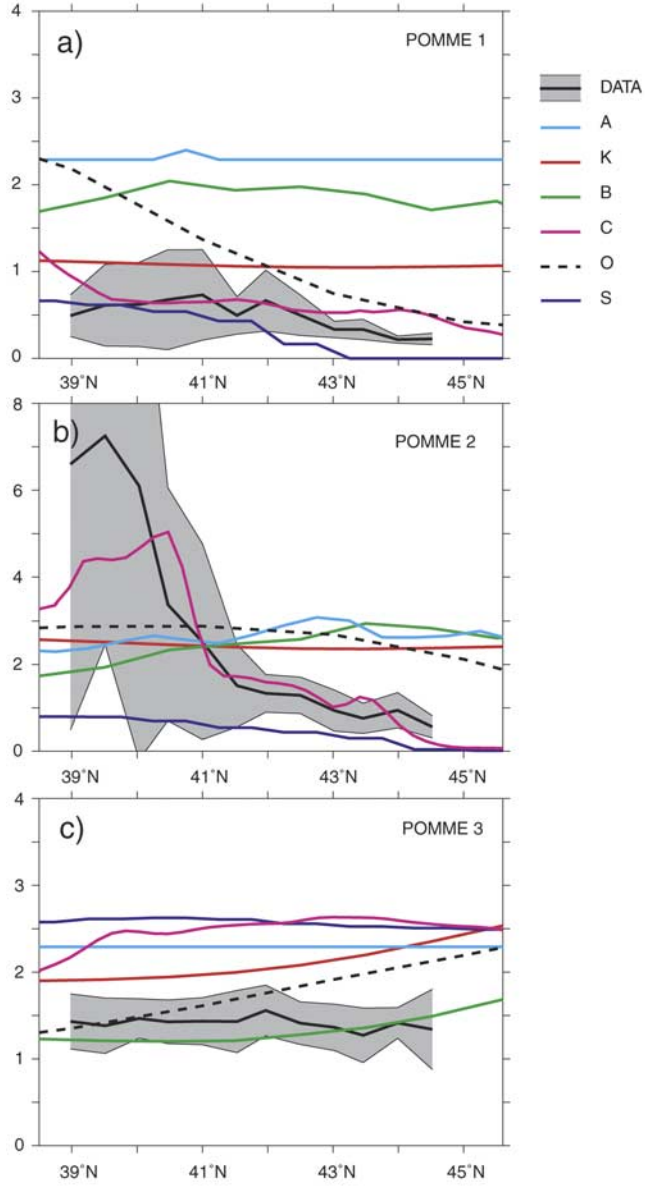

Figure 5. Latitudinal variability in the POMME area for observed DMS concentration, plotted as the mean (solid black line) and range (shaded area) of the discrete measurements carried out every $^1/_2$ degree of latitude, versus zonal means for 16°W–21°W from the different climatologies during (a) February 2001, (b) March–April 2001, and (c) August–September 2001.

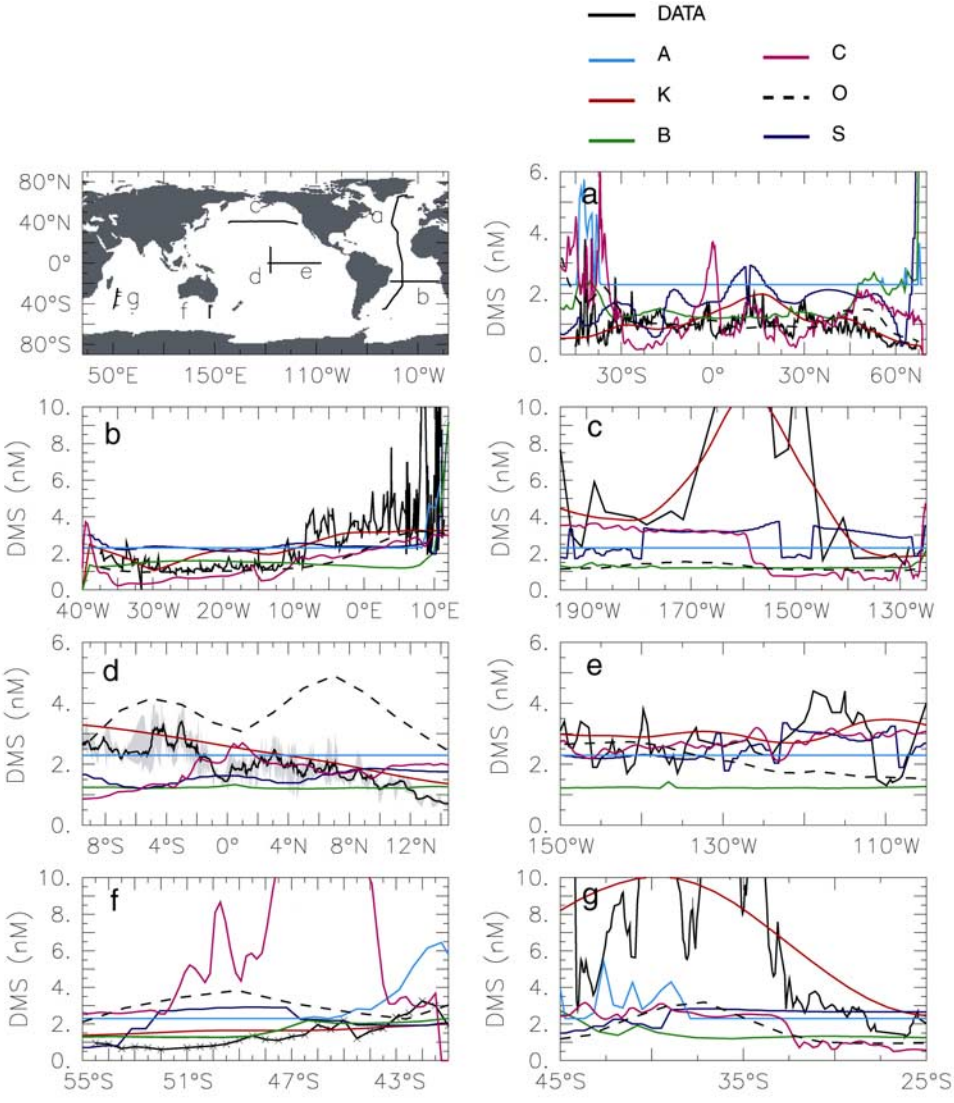

Figure 7. Variations of surface DMS (nmol L^{-1}) along different cruise tracks.

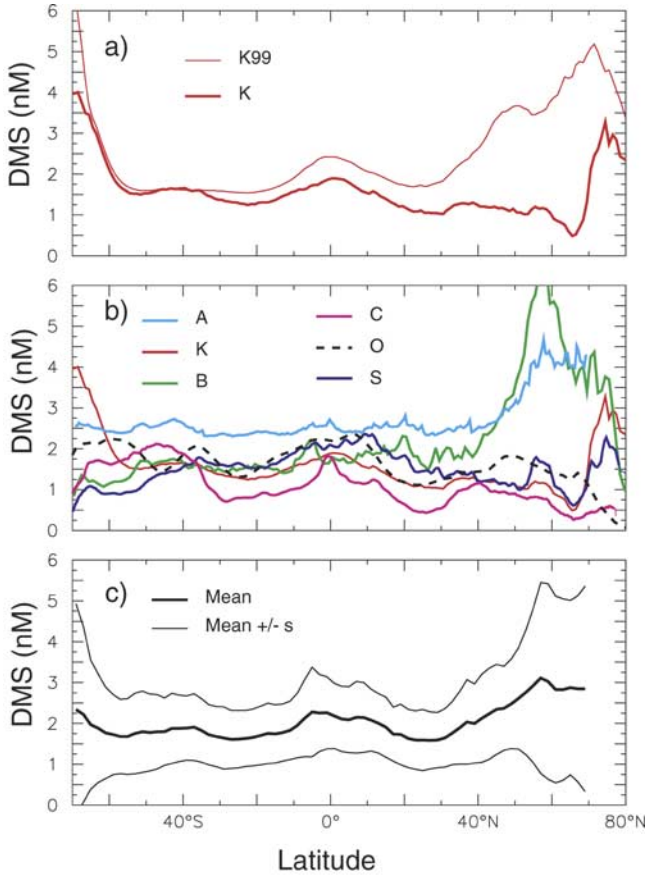

Figure 8. Summary of climatological zonal annual means of sea surface DMS: (a) Sensitivity of the climatology of *Kettle et al.* [1999] to data updating. (b) Intercomparison of the six climatologies. (c) Mean $\pm 1\sigma$ for the six climatologies.